Food Chemistry: X 25 (2025) 102247

Contents lists available at ScienceDirect

Food Chemistry: X

journal homepage: www.sciencedirect.com/journal/food-chemistry-x

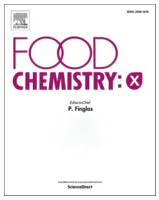

Efficient production of poly-γ-glutamic acid using computational fluid dynamics simulations by *Bacillus velezensis* for frozen dough bread making

Hong Liu [a], Qiaojuan Yan [a,*], Yuchuan Wang [b], Yanxiao Li [a,c], Zhengqiang Jiang [b,*]

[a] Key Laboratory of Food Bioengineering (China National Light Industry), College of Engineering, China Agricultural University, Beijing 100083, China
[b] Department of Nutrition and Health, College of Food Science & Nutritional Engineering, China Agricultural University, Beijing 100083, China
[c] Food Laboratory of Zhongyuan, Luohe 462000, Henan, China

ARTICLE INFO

Keywords:
Poly-γ-glutamic acid
Bacillus velezensis
Fed-batch fermentation
Computational fluid dynamics
Frozen dough
Bread

ABSTRACT

This study aimed to evaluate poly-γ-glutamic acid (γ-PGA) production by the glutamic-dependent strain *Bacillus velezensis* CAU263 through fed-batch fermentation in a 5-L fermenter. A remarkable γ-PGA yield of 60.4 g/L with a conversion rate of 0.97 g/g (γ-PGA/L-sodium glutamate) was achieved. To further enhance the γ-PGA yield, computational fluid dynamics (CFD) simulations were performed to optimize impeller combinations. With the adoption of six-semicircular blade Rushton turbine and four-skewed wide blade impellers (with a 20 % increase in impeller diameter), *B. velezensis* CAU263 produced a staggering 80.7 g/L of γ-PGA with a conversion rate of 1.29 g/g (γ-PGA/L-sodium glutamate). Furthermore, γ-PGA greatly improved the fermentation properties of frozen dough, yielding a 21.3 % increase in the specific volume of frozen dough bread and a remarkable 38.3 % reduction in hardness. Therefore, an efficient strategy for *B. velezensis* producing γ-PGA was provided, and the γ-PGA has tremendous potential as a cryoprotectant agent in the baking industry.

1. Introduction

Poly-γ-glutamic acid (γ-PGA) is a high value-added anionic biopolymer composed of D-glutamic acid and/or L-glutamic acid units connected by γ-amide linkages (Abdelnaby et al., 2024). Owing to its excellent characteristics such as biodegradability, water-solubility, biocompatibility, edibility, and environmental friendliness, γ-PGA has been applied in the industrial fields of food, cosmetics, agriculture, medicine, and environmental protection (Elbanna et al., 2024). With the widespread application of γ-PGA, many studies have focused on enhancing microbial production of this biopolymer (Parati et al., 2022). *Bacillus* species are particularly renowned for their excellent γ-PGA production because of their simple nutritional requirements, rapid growth rates, and high production efficiency, all of which are essential for γ-PGA production on industrial scale (Li, Hou, et al., 2022). The yield, molecular weight, and stereochemical composition of γ-PGA vary significantly depending on *Bacillus* species and cultivation conditions (Nair et al., 2023). These differences in molecular weight and stereochemical composition can be exploited in diverse industrial applications (Wang et al., 2022).

During fermentation, γ-PGA usually induces high viscosity of the fermentation broth (Parati et al., 2022). This elevated viscosity significantly hampers mass transfer, dissolved oxygen levels, and heat transfer within the fermentation broth, thus limiting further enhancement of γ-PGA production (Sirisansaneeyakul et al., 2017). Traditional scaling-up fermentation relies on collecting data from laboratory and pilot-scale experiments (Chen, Yi, et al., 2023). Nevertheless, this method is time-consuming and economically demanding. To address the limitations of experimental constraints in terms of time and complexity, computational fluid dynamics (CFD) simulations have emerged as an effective method for studying the fermenter structure and fluid characteristics (Nadal-Rey et al., 2022). The size and type of impeller significantly influence flow patterns with an optimal impeller combination, benefiting mixing and mass transfer properties (Bernauer et al., 2022). Verma et al. (2019) demonstrated that Rushton-marine impeller combination outperformed Rushton-Rushton impeller combination in terms of mixing and mass transfer performance, resulting in a 38.46 % higher microalgae concentration. However, the mediating effect of impeller size and type on the γ-PGA yield reduction caused by increased viscosity is unclear.

γ-PGA is a promising food ingredient (Abdelnaby et al., 2024). It plays an important role as a stabilizer and texture enhancer, enriching the taste and texture of baked goods, frozen foods, and beverages (Parati et al., 2022). γ-PGA can effectively deter ice crystal growth and

* Corresponding authors.
E-mail addresses: yanqj@cau.edu.cn (Q. Yan), zhqjiang@cau.edu.cn (Z. Jiang).

https://doi.org/10.1016/j.fochx.2025.102247
Received 24 October 2024; Received in revised form 14 January 2025; Accepted 27 January 2025
Available online 28 January 2025

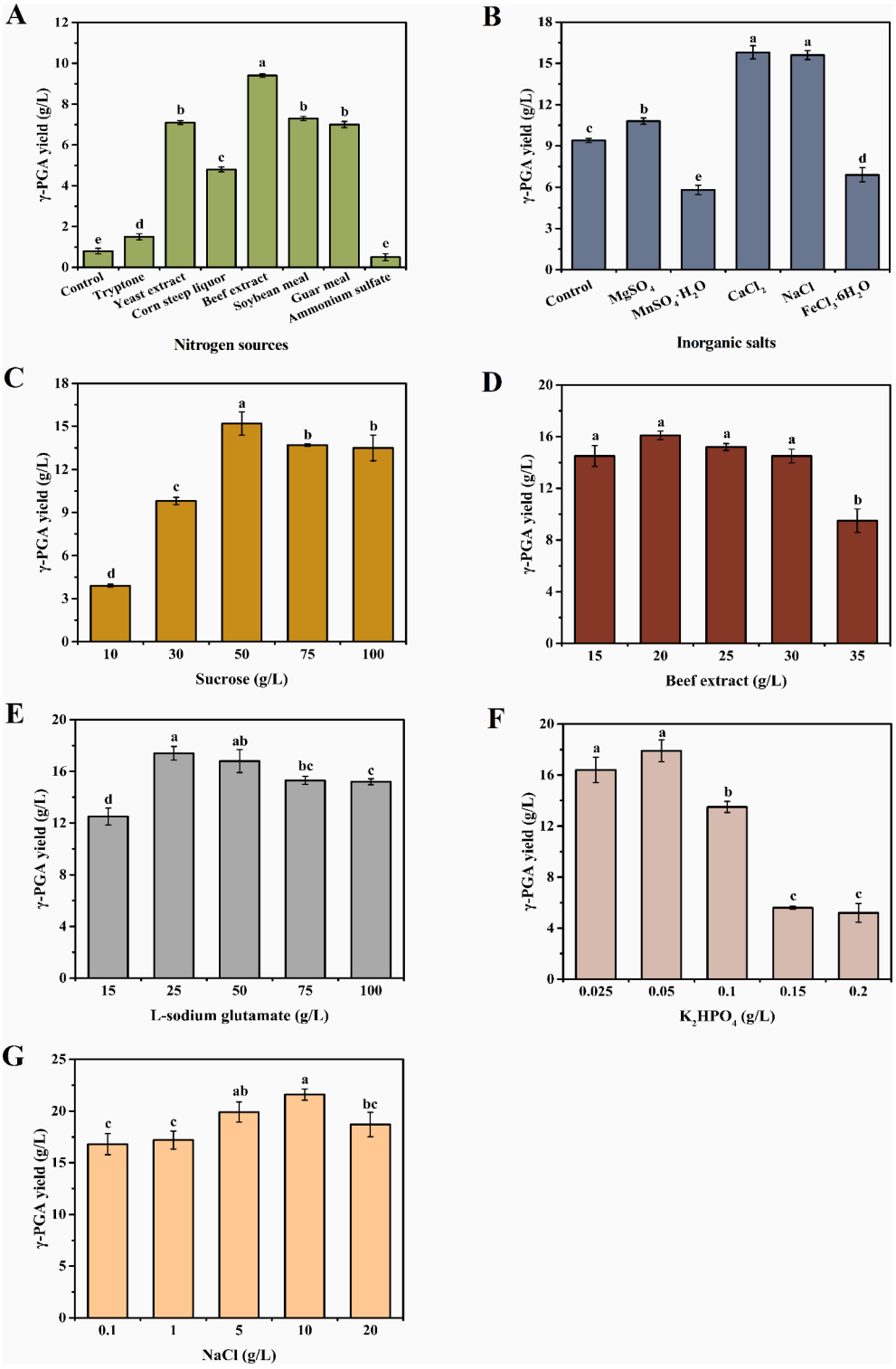

Fig. 1. Optimization of fermentation medium for γ-PGA production by *B. velezensis* CAU263 in shake flasks. (A) Effects of various nitrogen sources on γ-PGA production. (B) Effects of different inorganic salts on γ-PGA production. (C) Effects of different sucrose concentrations on γ-PGA production. (D) Effects of various beef extract concentrations on γ-PGA production. (E) Effects of different L-sodium glutamate concentrations on γ-PGA production. (F) Effects of K_2HPO_4 concentrations on γ-PGA production. (G) Effects of NaCl concentrations on γ-PGA production. Fermentation was conducted at 37 °C for 48 h.

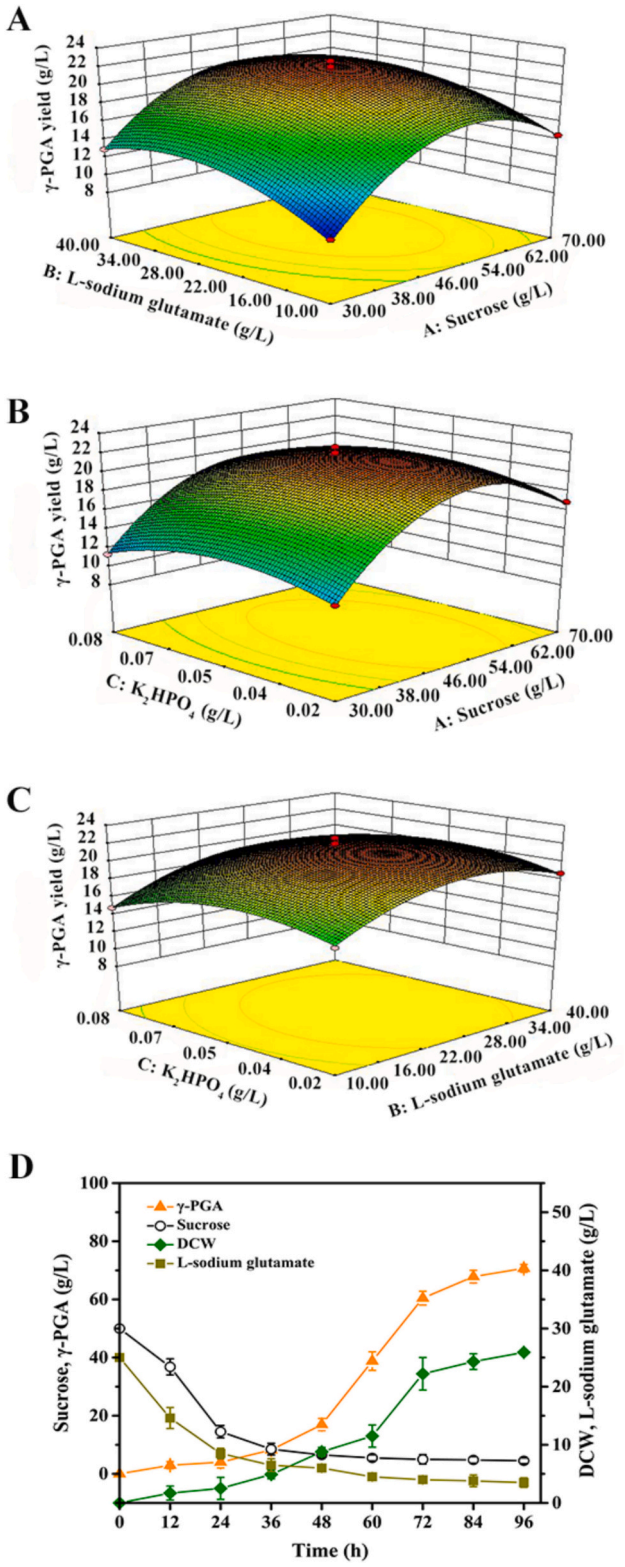

Fig. 2. Response surface and contour plots of sucrose and L-sodium glutamate (A), sucrose and K_2HPO_4 (B), L-sodium glutamate and K_2HPO_4 (C), and time course via fed-batch fermentation in a 5-L fermenter (D) for γ-PGA production by *B. velezensis* CAU263. Fermentation was performed at 37 °C with stirring at 400 rpm and an airflow of 1.5 vvm for 96 h. NH_4OH or H_3PO_4 was automatically added to maintain pH 7.0. The feeding medium (500 g/L sucrose, 200 g/L beef extract, and 250 g/L L-sodium glutamate) was fed into the fermenter when the sucrose concentration dropped below 10 g/L, and the agitation rate was adjusted to 600 rpm.

recrystallization in frozen dough (Yokoigawa et al., 2006). Additionally, it can protect baker's yeast and improve the leavening capability of frozen dough, resulting in an increased specific volume of frozen dough bread (Jia et al., 2016). In our previous study, *B. velezensis* CAU263, a high-yield producer of γ-PGA (155.1 g/kg via solid-state fermentation), was successfully isolated from traditional Chinese *Douchi* (Liu et al., 2022). In this study, a systematic optimization and CFD simulations strategy were employed to enhance γ-PGA production by *B. velezensis* CAU263. Furthermore, the effect of γ-PGA on the quality of frozen dough bread was evaluated.

2. Materials and methods

2.1. Microorganisms and cultivation

In this study, *B. velezensis* CAU263 (CGMCC No: 20318) was used as the γ-PGA producer (Liu et al., 2022). *B. velezensis* CAU263 was inoculated into a 50 mL shake flask containing 10 mL of LB medium. The flask was incubated at 37 °C for 12 h, with continuous agitation at 200 rpm. Subsequently, the seed culture (5 %, *v/v*) was inoculated into a 250 mL shake flask containing 30 mL of basal fermentation medium (50 g/L sucrose, 75 g/L L-sodium glutamate, and 0.025 g/L K_2HPO_4). The flask was then incubated at 37 °C for 48 h with continuous agitation at 200 rpm.

2.2. Optimization of γ-PGA production in shake flasks

The effects of seven nitrogen sources (soybean meal, guar meal, yeast extract, beef extract, tryptone, corn steep liquor, and ammonium sulfate) and five inorganic salts ($CaCl_2$, NaCl, $MgSO_4$, $MnSO_4•H_2O$, and $FeCl_3•6H_2O$) on γ-PGA production were optimized using a one-factor-at-a-time approach. The concentrations of each nitrogen source and inorganic salt were set to 15 g/L and 0.1 g/L, respectively. Under the above optimized medium, the quantity of each medium component was investigated. Moreover, response surface methodology (RSM) was employed to optimize the concentrations of three key factors (sucrose, L-sodium glutamate and K_2HPO_4) for γ-PGA production using a Box-Behnken design (BBD). Seventeen experiments of three factors at three levels were carried out (Table S1). The results and the coefficients of the quadratic equation were analyzed using the analysis of variance (ANOVA) by Design-Expert 8.0.6. The resulting optimal fermentation medium was used for subsequent experiments.

2.3. Production of γ-PGA in a 5-L fermenter

Fed-batch fermentation of *B. velezensis* CAU263 was performed in a 5-L fermenter containing 2 L of medium (inoculum size of 10 %, *v/v*). The optimized medium composition comprised 50 g/L sucrose, 20 g/L beef extract, 25 g/L L-sodium glutamate, 0.1 g/L $CaCl_2$, 0.05 g/L K_2HPO_4, and 10 g/L NaCl. The cultivation process was conducted by incubation at 37 °C with stirring at 400 rpm and an airflow rate of 1.5 vvm for 96 h. To maintain a pH of 7.0, NH_4OH or H_3PO_4 was automatically added. A medium containing 500 g/L sucrose, 200 g/L beef extract, and 250 g/L L-sodium glutamate was fed into the fermenter, as long as the sucrose content remained below 10 g/L, with the agitation speed adjusted to 600 rpm. Samples were collected every 12 h to monitor the biomass, sucrose concentration, L-sodium glutamate concentration, and γ-PGA yield.

2.4. Purification and characterization of γ-PGA

The supernatant was obtained by centrifugation of the fermentation broth at 10000 rpm for 20 min. Subsequently, γ-PGA was purified using a previously established method (Liu et al., 2022). Purified γ-PGA was evaluated by thin-layer chromatography (TLC) in accordance with the procedure described by Ali et al. (2020). Simultaneously, the

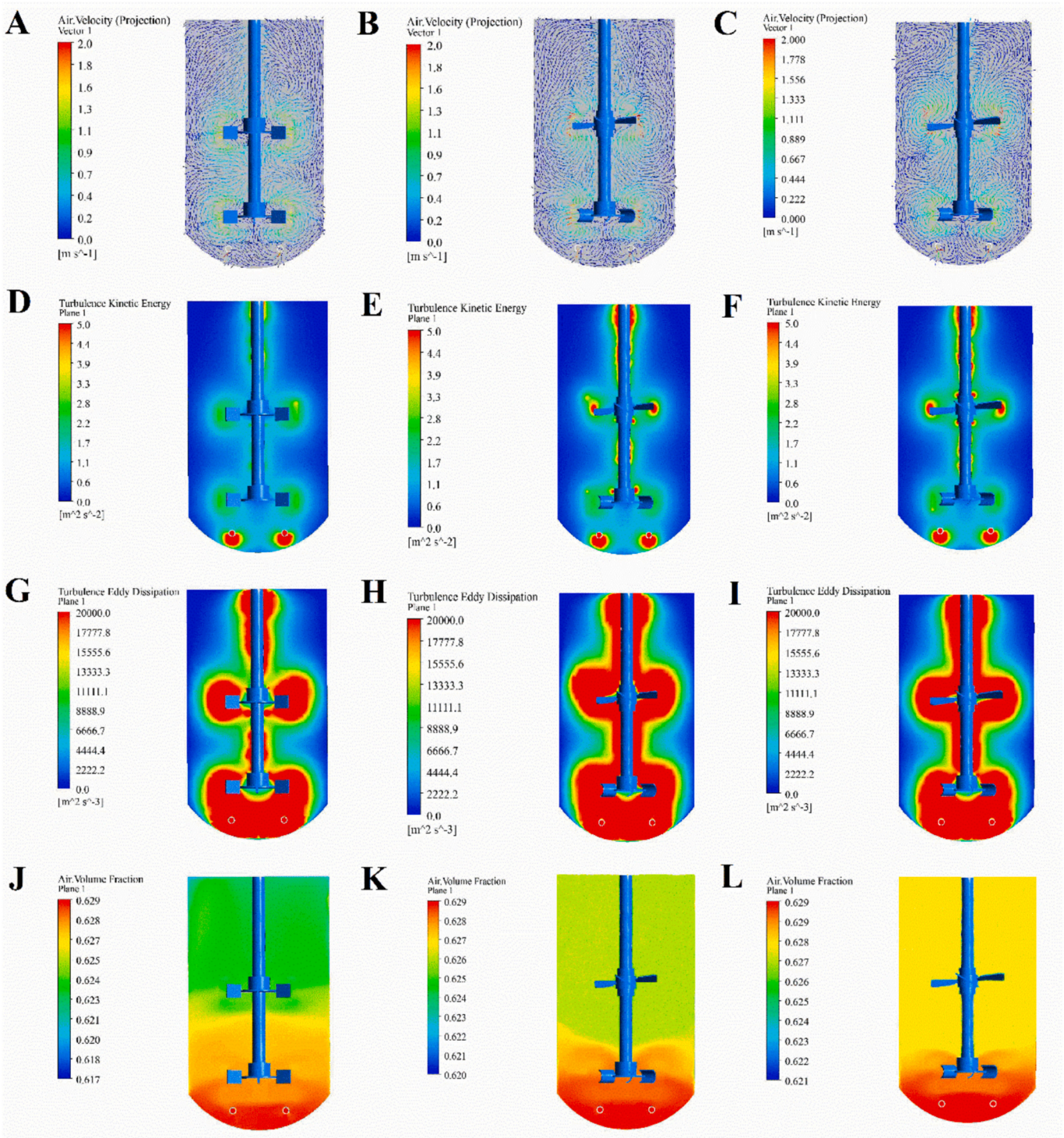

Fig. 3. Fluid properties of three impeller combinations in a 5-L fermenter. (A–C) Velocity vectors, (D—F) turbulent kinetic energy, (G–I) eddy dissipation rate, and (J–L) gas volume fractions for the six-straight blade Rushton turbine impeller combination, six-semicircular blade Rushton turbine impeller and four-skewed wide blade impeller combination, and six-semicircular blade Rushton turbine impeller and four-skewed wide blade impeller (with a 20 % increase in impeller diameter) combination.

stereochemical composition of γ-PGA was determined by high-performance liquid chromatography (HPLC) (Kongklom et al., 2017). Furthermore, the weight-average molecular weight (Mw) was determined using gel permeation chromatography (GPC) (Halmschlag et al., 2019).

2.5. Determination of γ-PGA and cell biomass

The concentration of γ-PGA was determined using cetyltrimethylammonium bromide (CTAB) turbidimetry method (Halmschlag et al., 2019). Dry cell weight (DCW) was used to assess cell biomass. Approximately 10 mL of the fermentation broth was

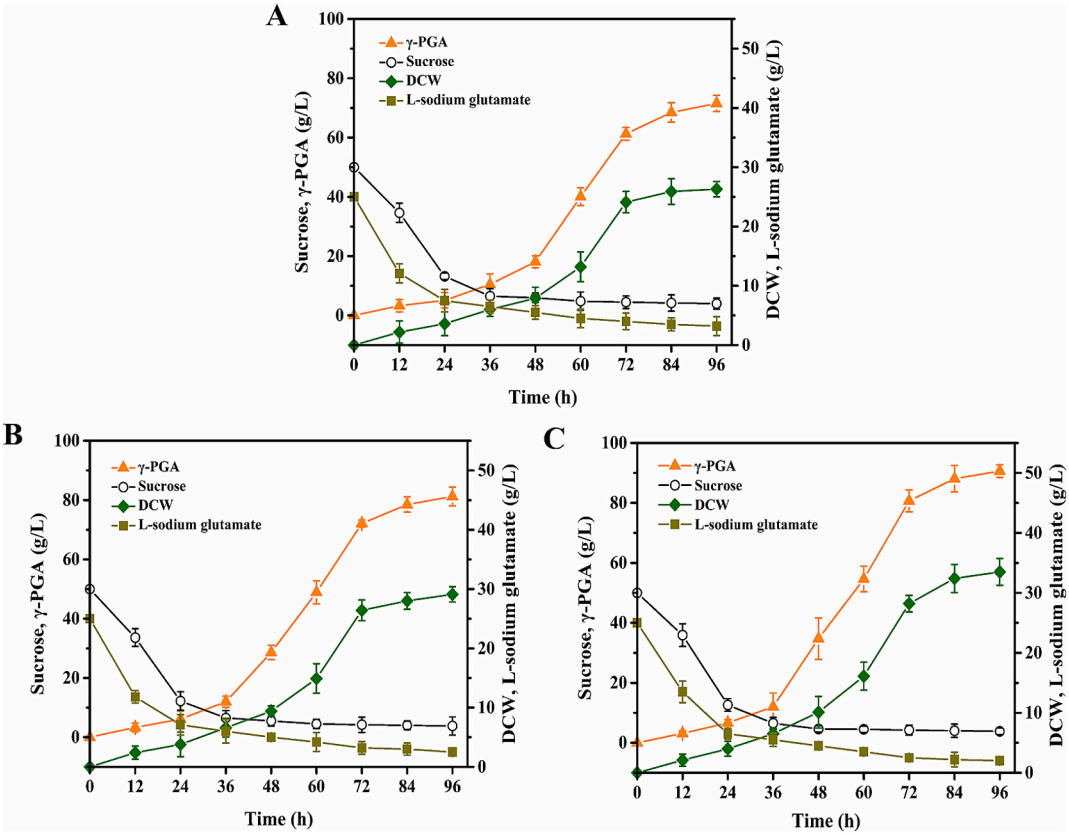

Fig. 4. Time course of γ-PGA production via fed-batch fermentation by *B. velezensis* CAU263 using three impeller combinations in a 5-L fermenter. (A) Time course of γ-PGA production by six-straight blade Rushton turbine impeller combination. (B) Time course of γ-PGA production by six-semicircular blade Rushton turbine impeller and four-skewed wide blade impeller combination. (C) Time course of γ-PGA production by six-semicircular blade Rushton turbine impeller and four-skewed wide blade impeller (with a 20 % increase in impeller diameter) combination. Fermentation was performed at 37 °C with stirring at 400 rpm and an airflow of 1.5 vvm for 96 h. NH_4OH or H_3PO_4 was automatically added to maintain a pH of 7.0. The feeding medium (500 g/L sucrose, 200 g/L beef extract, and 250 g/L L-sodium glutamate) was fed into the fermenter when the sucrose concentration dropped below 10 g/L, and the agitation rate was adjusted to 600 rpm.

centrifuged at 10000 rpm for 20 min. After two washes with distilled water, the cell precipitate was dried until a constant weight was obtained.

2.6. Determination of residual sucrose and L-sodium glutamate

Sucrose concentration was assessed using a sucrose detection kit (Nanjing Jiancheng Bioengineering Institute, China). L-sodium glutamate concentration was analyzed using an SBA-40C bioanalyzer (Shandong Academy of Sciences, China).

2.7. CFD simulations of impeller combinations in a 5-L fermenter

2.7.1. Geometrical model

The geometric specifications of the 5-L fermenter are shown in Fig. S1. The fermenter was 280 mm in height and 160 mm in diameter. It features four baffles, each measuring 230 mm × 16 mm, with a gas distributor diameter of 60 mm. The gas distributor consisted of eight gas holes, each with a diameter of 0.8 mm. The fermenter was mechanically stirred using a two-stage impeller. The initial impeller combination consisted of a six-straight blade Rushton turbine paired with a six-straight blade Rushton turbine. Subsequently, a radial flow impeller six-semicircular blade Rushton turbine and an axial flow impeller four-skewed wide blade were adopted to optimize impeller combinations. Three sets of impeller combinations (six-straight blade Rushton turbine and six-straight blade Rushton turbine, six-semicircular blade Rushton turbine and four-skewed wide blade, six-semicircular blade Rushton turbine and four-skewed wide blade (with a 20 % increase in impeller diameter)) were designed to investigate the impact of impeller size and combination on the flow field properties. These configurations are illustrated in Fig. S1 and are detailed in Table S2.

2.7.2. CFD model setup

The simulations were performed using ANSYS Fluent software (ANSYS Inc., USA), and the meshes were created using ANSYS Fluent Meshing software version 2020 R1. The gas-liquid flow was simulated using the Euler-Euler two-phase model. The turbulence in the fermenter was simulated using the standard κ-ε model in conjunction with the standard wall function. Impeller rotation was simulated using the multiple reference frame (MRF) approach. The inlet and outlet of the fermentation model were identified as the openings of the gas distributors and free top surface of the fermenter, respectively, with velocity inlet and degassing as their boundary conditions. The impellers and stirring shaft were designated as moving walls, whereas the remaining walls were maintained static by default. Additionally, no-slip boundary conditions were specified for all walls (Nadal-Rey et al., 2022).

2.8. Cryoprotective effects of γ-PGA on frozen dough bread quality

2.8.1. Preparation of frozen dough and bread

The dough recipe consisted of 700 g wheat flour, 56 g sugar, 7 g salt, 14 g yeast, 378 mL water, and 28 g butter. Prior to mixing, varying amounts of γ-PGA were incorporated into the flour at concentrations of 0, 0.1, 0.2, 0.3, 0.4, 0.5, and 0.6 g/kg flour. Dough was prepared using the method described by Liu et al. (2022). Afterward, the dough was rapidly frozen in a − 80 °C refrigerator for 20 min and subsequently

Table 1
Effects of frozen storage time and γ-PGA concentration on freezable water content of frozen dough.

Frozen Storage Time (week)	γ-PGA (g/kg)	ΔH (J/g)	FW (%)	NFW (%)
2	0	64.3 ± 1.12^{a}	45.9 ± 0.09^{a}	54.1 ± 0.15^{d}
	0.1	60.4 ± 0.98^{b}	43.0 ± 0.18^{b}	57.0 ± 1.39^{cd}
	0.2	57.9 ± 0.05^{c}	41.2 ± 0.32^{bc}	58.8 ± 1.14^{bc}
	0.3	54.5 ± 0.28^{d}	38.9 ± 0.75^{cd}	61.1 ± 0.58^{ab}
	0.4	50.6 ± 0.39^{e}	36.0 ± 1.28^{e}	64.0 ± 0.62^{a}
	0.5	51.6 ± 1.37^{e}	36.8 ± 1.92^{de}	63.2 ± 0.29^{a}
	0.6	55.3 ± 0.86^{d}	39.4 ± 0.17^{c}	60.6 ± 2.78^{abc}
4	0	68.6 ± 2.75^{a}	48.9 ± 0.66^{a}	51.1 ± 0.05^{c}
	0.1	64.4 ± 0.31^{b}	45.9 ± 3.25^{ab}	54.1 ± 1.59^{b}
	0.2	61.4 ± 1.24^{bc}	43.8 ± 0.01^{bc}	56.2 ± 1.48^{ab}
	0.3	59.9 ± 0.06^{cd}	42.7 ± 0.11^{bc}	57.3 ± 0.36^{a}
	0.4	57.7 ± 0.12^{d}	41.1 ± 1.46^{c}	58.9 ± 0.17^{a}
	0.5	58.9 ± 0.18^{cd}	42.0 ± 1.39^{bc}	58.0 ± 1.61^{a}
	0.6	61.0 ± 0.25^{c}	43.5 ± 0.83^{bc}	56.5 ± 0.08^{ab}

Data are expressed as mean ± standard deviation ($n = 3$). Values with different superscript lowercase letters in the same column of the same frozen storage time indicate significant differences ($p < 0.05$). ΔH represents enthalpy of melting, FW represents freezable water content, NFW represents non-freezable water content.

stored in a − 20 °C refrigerator for 2 and 4 weeks (Shu et al., 2022).

After thawing at 4 °C, the frozen dough fermented for 60 min at 38 °C with 80 % relative humidity before baking (surface temperature 180 °C, bottom temperature 200 °C, 20 min).

2.8.2. Yeast viability measurement

The yeast cell suspension was evenly spread on YPD plates and cultivated at 30 °C for 48 h after thawing the frozen dough. Yeast viability was determined by quantifying the viable yeast cell count before and after freezing (Yokoigawa et al., 2006).

2.8.3. Fermentation capacity measurement of frozen dough

The fermentation capacity of 200 g of thawed frozen dough, equipped with a 2 kg cylindrical weight, was measured using a Rheofermentometer F4 (Chopin, Paris, France). The experiment was conducted for 3 h at 38 °C (Liu et al., 2018).

2.8.4. Freezable water content determination of frozen dough

The freezable water content of frozen dough was assessed using the method developed by Zhu et al. (2022).

2.8.5. Rheological measurement of frozen dough

The rheological properties of frozen dough were examined using the method proposed by Lin et al. (2021).

2.8.6. Scanning electron microscopy (SEM) observation of frozen dough

The microstructure of frozen dough was observed based on the method described by Liu et al. (2018).

2.8.7. Specific volume and texture profile analyses of frozen dough bread

The specific volume and textural properties of the bread were measured using the method described by Liu et al. (2022), after cooling for 2 h at 25 °C.

2.8.8. Moisture distribution measurement of frozen dough bread

Moisture distribution in frozen dough bread was determined using low-field nuclear magnetic resonance (LF-NMR), following the method reported by Yang et al. (2022).

2.9. Statistical analysis

All data are presented as the mean ± standard deviation of three replicates. Statistical analysis was performed using SPSS 16.0 and Origin 9.2, with a significance level of $p < 0.05$.

3. Results and discussion

3.1. Fermentation medium optimization for γ-PGA production

As shown in Fig. 1A, all tested nitrogen sources were utilized by *B. velezensis* CAU263 to produce γ-PGA. The highest γ-PGA yield, reaching 9.4 g/L, was achieved when the beef extract was used as the nitrogen source. In Fig. 1B, the impact of inorganic salts on γ-PGA production is depicted, with $CaCl_2$ and NaCl resulting in γ-PGA yields of 15.8 g/L and 15.6 g/L, respectively. Maintaining a sucrose concentration of 50 g/L yielded the highest γ-PGA production of 15.2 g/L (Fig. 1C). Maximal γ-PGA concentration of 16.1 g/L was attained with 20 g/L beef extract (Fig. 1D). As shown in Fig. 1E, L-sodium glutamate addition at 25 g/L led to the highest γ-PGA yield of 17.4 g/L. Further improvements were observed at different concentrations of K_2HPO_4 (Fig. 1F), where the highest γ-PGA concentration of 17.9 g/L was achieved with the addition of 0.05 g/L K_2HPO_4. Additionally, a maximum γ-PGA yield of 21.6 g/L was obtained using 10 g/L NaCl (Fig. 1G). Based on these results, the optimal fermentation medium consisted of 50 g/L sucrose, 20 g/L beef extract, 25 g/L L-sodium glutamate, 0.1 g/L $CaCl_2$, 0.05 g/L K_2HPO_4, and 10 g/L NaCl. Moreover, the optimization of sucrose (A), L-sodium glutamate (B) and K_2HPO_4 (C) was further performed by RSM to enhance γ-PGA production by *B. velezensis* CAU263. The ANOVA (analysis of variance) result is shown in Table S3. The model was highly significant as the "Model p value" (<0.0001). Among the model terms, A, B, C, AB, A^2, B^2, C^2 independently showed their significance. The regression analysis was followed by a second-order polynomial equation model as follows:

$$Y = 21.78 + 2.03 \times A + 1.29 \times B - 0.61 \times C - 0.60 \times A \times B - 0.25 \times A \times C + 0.13 \times B \times C - 5.85 \times A^2 - 2.83 \times B^2 - 2.08 \times C^2.$$

The interaction effects among the three variables were visualized using response surface plots (Fig. 2A–2C). The predicted maximum yield of γ-PGA was 22.1 g/L under optimal conditions: 53.3 g/L sucrose, 28.1 g/L L-sodium glutamate and 0.05 g/L K_2HPO_4. Validation experiments under these conditions yielded a maximum γ-PGA production of 21.5 ± 0.33 g/L, which closely aligned with the predicted value.

Seven different nitrogen sources and four types of mineral salts were selected to assess their potential for γ-PGA production in shake flasks. Among the nitrogen sources investigated, only organic nitrogen sources were utilized effectively by *B. velezensis* CAU263. Notably, the beef extract exhibited the highest yield of γ-PGA. In contrast, inorganic nitrogen sources, such as ammonium sulfate, were unsuitable for both γ-PGA formation and cell growth. This nitrogen sources preference exhibited by *B. velezensis* CAU263 mirrors that of other strains such as *B. methylotrophicus* SK19.001 (Peng et al., 2015), *Bacillus* sp. FBL-2 (Min et al., 2019), and *B. subtilis* GXD-20 (Zeng et al., 2024). Nevertheless,

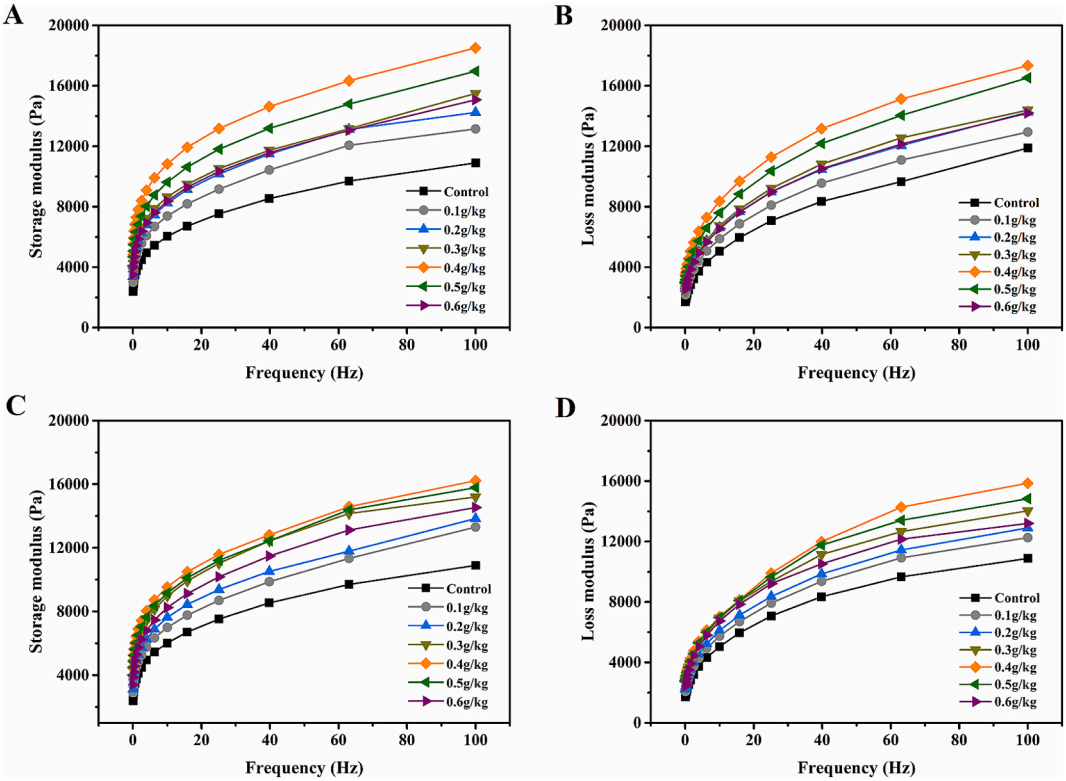

Fig. 5. Effects of frozen storage time and γ-PGA concentration on the rheological properties of frozen dough.

strains such as *B. amyloliquefaciens* NX-2S (Qiu et al., 2017), *B. siamensis* IR10 (Wang et al., 2020), and *B. licheniformis* A14 (Ali et al., 2020) show a preference for inorganic nitrogen sources for γ-PGA production. These findings indicate that the selection of a nitrogen source is typically strain-dependent, with no universally applicable source (Min et al., 2019). Mineral salts, essential components of culture media, play a crucial role in cell growth and γ-PGA yield (Li, Hou, et al., 2022). In this study, the addition of $CaCl_2$ and NaCl significantly enhanced γ-PGA production. It is plausible that $CaCl_2$ and NaCl may positively affect enzymatic reactions involved in γ-PGA synthesis during bacterial metabolism (Ratha & Jhon, 2019). Conversely, $MnSO_4{\cdot}H_2O$ and $FeCl_3{\cdot}6H_2O$ were found to notably inhibit γ-PGA production.

3.2. Production of γ-PGA by fed-batch fermentation

Fed-batch fermentation was performed in a 5-L fermenter to enhance the yield of γ-PGA produced by *B. velezensis* CAU263 (Fig. 2D). At 72 h, the γ-PGA yield reached 60.4 g/L with a productivity of 0.84 g/L/h. The conversion rates were 0.48 g/g (γ-PGA/sucrose) and 0.97 g/g (γ-PGA/L-sodium glutamate).

Numerous studies have explored fed-batch fermentation of γ-PGA, often utilizing *B. subtilis* and *B. licheniformis* for industrial production (Nair et al., 2023). Typically, the reported yield and productivity of γ-PGA fall within the range of 32.1–101.1 g/L and 0.67–2.20 g/L/h, respectively. The conversion rate is in the range of 0.99–3.37 (γ-PGA/L-sodium glutamate). Compared to previous reports (Huang et al., 2011; Kongklom et al., 2017; Li, Chen, et al., 2022), the yield and productivity of γ-PGA in this study fell within the upper-middle range, with a medium conversion rate of L-sodium glutamate to γ-PGA. However, the high viscosity of the fermented solution in this study hindered the oxygen transmission efficiency, affecting nutrients transfer and oxygen distribution (Sirisansaneeyakul et al., 2017; Song et al., 2019). The subsequent aim is to enhance the mass transfer efficiency, and CFD can aid in optimizing impeller design.

3.3. CFD simulations for γ-PGA production in a 5-L fermenter

When employing the four-skewed wide blade impeller, the axial jet formed loops that exited the sides of the fermenter. In contrast, when using the six-straight blade Rushton turbine and six-semicircular blade Rushton turbine impellers, the radial jet created loops that also exited the sides of the fermenter (Fig. 3A–3C). The combination of six-semicircular blade Rushton turbine and four-skewed wide blade impellers (with an increased impeller diameter of 20 %) achieved a higher range distribution of turbulent kinetic energy and gas volume fractions compared to the other two impeller combinations (Fig. 3D–3F and 3J–3L). In regions near the impellers, higher local values of the eddy dissipation rate were observed with the six-semicircular blade Rushton turbine and four-skewed wide blade impellers than with the six-straight blade Rushton turbine impeller (Fig. 3G–3I).

The fed-batch fermentation employing six-straight blade Rushton turbine impeller combination resulted in a γ-PGA yield of 61.3 g/L with a conversion rate of 0.98 g/g (γ-PGA/L-sodium glutamate) achieved at 72 h (Fig. 4A). Meanwhile, the fed-batch fermentation utilizing a combination of six-semicircular blade Rushton turbine and four-skewed wide blade impellers yielded a γ-PGA titer of 72.1 g/L with a conversion rate of 1.15 g/g (γ-PGA/L-sodium glutamate) (Fig. 4B). Furthermore, when employing a combination of six-semicircular blade Rushton turbine impeller and four-skewed wide blade impeller (with an increased impeller diameter of 20 %), the γ-PGA yield reached 80.7 g/L, and the conversion rate was up to 1.29 g/g (γ-PGA/L-sodium glutamate) (Fig. 4C). The purified products from *B. velezensis* CAU263 consisted entirely of glutamic acid (Fig. S2A), with a Mw of 3.3×10^6 Da (Fig. S2B), and the purity of γ-PGA was 92.1 %. In terms of the stereochemical composition, they contained 42.5 % L-glutamic acid and 57.5 % D-glutamic acid (Fig. S2C).

A comparison of γ-PGA fermentation by *B. velezensis* CAU263 with that in other studies is shown in Table S4. The highest reported γ-PGA productivity, as presented by Huang et al. (2011), was 2.20 g/L/h (101.1 g/L γ-PGA) using fed-batch fermentation in a 10 L fermenter with

Table 2
Effects of frozen storage time and γ-PGA concentration on rheofermentation parameters of frozen dough.

Frozen Storage Time (week)	γ-PGA (g/kg)	Hm (mm)	h (mm)	A_T (mL)	A_1 (mL)	R (%)
2	0	38.2 ± 0.58^{d}	34.6 ± 0.22^{d}	1445 ± 30.55^{e}	1150 ± 18.85^{e}	79.6 ± 1.21^{d}
	0.1	39.5 ± 0.23^{d}	35.2 ± 0.75^{d}	1642 ± 28.21^{d}	1332 ± 15.45^{d}	81.1 ± 0.77^{cd}
	0.2	41.1 ± 1.12^{c}	36.9 ± 0.68^{c}	1655 ± 19.88^{cd}	1375 ± 25.18^{c}	83.1 ± 0.83^{c}
	0.3	43.3 ± 0.92^{b}	38.1 ± 1.24^{bc}	1687 ± 20.53^{bc}	1446 ± 24.37^{b}	85.7 ± 1.58^{b}
	0.4	45.9 ± 1.35^{a}	39.8 ± 0.55^{a}	1710 ± 21.21^{ab}	1510 ± 22.23^{a}	88.4 ± 1.92^{a}
	0.5	46.4 ± 0.65^{a}	38.5 ± 0.82^{ab}	1715 ± 18.74^{ab}	1478 ± 31.25^{ab}	86.2 ± 1.34^{ab}
	0.6	47.1 ± 0.18^{a}	37.1 ± 1.01^{bc}	1737 ± 15.65^{a}	1439 ± 29.16^{b}	82.8 ± 0.78^{c}
4	0	35.5 ± 0.42^{e}	32.5 ± 0.38^{d}	1380 ± 23.82^{e}	1046 ± 23.40^{d}	75.8 ± 0.99^{d}
	0.1	38.3 ± 0.57^{d}	34.7 ± 0.71^{c}	1594 ± 17.54^{d}	1277 ± 27.22^{c}	80.1 ± 1.57^{c}
	0.2	38.9 ± 1.11^{d}	35.0 ± 0.28^{c}	1621 ± 24.75^{cd}	1318 ± 18.85^{c}	81.3 ± 2.01^{bc}
	0.3	40.5 ± 0.63^{c}	36.8 ± 1.05^{ab}	1646 ± 22.81^{bc}	1374 ± 17.48^{b}	83.5 ± 1.86^{ab}
	0.4	42.9 ± 0.98^{b}	37.9 ± 0.98^{a}	1675 ± 17.50^{ab}	1436 ± 12.91^{a}	85.7 ± 0.72^{a}
	0.5	43.2 ± 1.02^{b}	37.5 ± 0.32^{ab}	1687 ± 22.63^{ab}	1420 ± 32.72^{a}	84.2 ± 1.05^{a}
	0.6	45.0 ± 0.88^{a}	36.6 ± 0.55^{b}	1711 ± 28.28^{a}	1372 ± 30.12^{b}	80.2 ± 1.79^{c}

Data are expressed as mean ± standard deviation (n = 3). Values with different superscript lowercase letters in the same column of the same frozen storage time indicate significant differences ($p < 0.05$).

B. subtilis ZJU-7, achieving a conversion rate of 3.37 g/g (γ-PGA/L-sodium glutamate). Notably, the yield and productivity of γ-PGA in this study closely resembled those reported by Huang et al. (2011). During the fermentation process, γ-PGA accumulation increases the viscosity of the fermentation broth, which hinders further improvements in γ-PGA yield (Parati et al., 2022). Various strategies have been developed to increase γ-PGA production, such as regulating the concentrations of NaCl, $CaCl_2$, and KCl (Zeng et al., 2016), incorporating oxygen carriers (Wang et al., 2020), employing a moving bed biofilm reactor (Jiang et al., 2016), and adjusting the γ-PGA hydrolase activity (Elbanna et al., 2024). γ-PGA hydrolases are directly involved in the degradation of γ-PGA to regulate the molecular weight of γ-PGA (Parati et al., 2022). PgdS hydrolases were able to increase the yields of γ-PGA, while the molecular weight was significantly decreased (Sha et al., 2019; Tian et al., 2014). This could be primarily attributed to the reduced viscosity of fermentation solution and increased oxygen distribution induced by PgdS, thus benefiting biomass growth and synthesis of γ-PGA (Fukushima et al., 2018; Guo et al., 2024). Furthermore, optimization of the stirring impeller using CFD offers several advantages, including cost-effectiveness, energy efficiency, and enhanced production efficiency (Nadal-Rey et al., 2022). As shown in Table S4, high levels of γ-PGA yield and productivity were achieved in this study using fed-batch fermentation with a combination of six-semicircular blade Rushton turbine impeller and four-skewed wide blade impeller (with an increased impeller diameter of 20 %). The conversion rate of L-sodium glutamate to γ-PGA was also notably high. These results can be attributed to the enhanced oxygen distribution and mass transfer efficiency resulting from the impeller optimization (Jiang et al., 2016; Chen, Yi, et al., 2023). The four-skewed wide blade impeller exhibited superior downward circulation energy compared to the six-straight blade Rushton turbine and six-semicircular blade Rushton turbine impellers, leading to a higher gas holdup capacity (Bernauer et al., 2022). The presence of air dead zones and large gas cavities behind the impeller blades hinders oxygen mass transfer, potentially decreasing fermentation efficiency (Nadal-Rey et al., 2022). The six-semicircular blade Rushton turbine impeller provided better gas dispersion and fewer gas cavities than the six-straight blade Rushton turbine impeller. Meanwhile, the four-skewed wide blade impeller excelled in gas dispersion and gas-liquid mixing (Verma et al., 2019; Chen, Yi, et al., 2023). Among the three impeller combinations, the six-semicircular blade Rushton turbine impeller and four-skewed wide blade impeller (with an increased impeller diameter of 20 %) displayed significant advantages in terms of gas volume fraction (Nadal-Rey et al., 2022). Consequently, the fermenter equipped with this combination demonstrated superior oxygen distribution and mass transfer efficiency compared with other combinations. The findings of this study highlight the potential applications of stirring impeller optimization and *B. velezensis* CAU263 in the industrial production of γ-PGA.

3.4. Cryoprotective effects of γ-PGA on frozen dough properties

The effect of γ-PGA from *B.velezensis* CAU263 on freezable water content is shown in Table 1. Specifically, the addition of 0.4 g/kg γ-PGA resulted in a remarkable decrease of 21.6 % and 16.0 % in the freezable water content after 2 and 4 weeks of freezing, respectively. Furthermore, the frozen dough containing γ-PGA demonstrated higher values of G' (storage modulus) and G" (loss modulus) compared to the control. Notably, the maximum values of G' and G" were achieved at a γ-PGA addition of 0.4 g/kg (Fig. 5). The effect of γ-PGA from *B.velezensis* CAU263 on yeast survival during frozen storage showed a concentration-dependent pattern (Fig. S3). After 2 weeks of freezing, yeast viability ranged from 21.5 % to 83.2 % with γ-PGA additions ranging from 0.1 g/kg to 0.6 g/kg. Even after 4 weeks of freezing, yeast cell viability remained above 50 % when γ-PGA was at 0.4 g/kg. Additionally, the fermentation capabilities of the frozen dough were evaluated using a Rheofermentometer F4 (Table 2). After 2 and 4 weeks of frozen storage, a 0.4 g/kg addition of γ-PGA led to a 18.3 % and 21.4 % increase in the total gas volume (A_T), respectively. Meanwhile, the gas retention volume (A_1) and gas retention ratio (R) increased by 31.3 % and 11.1 % after 2 weeks, and by 37.3 % and 13.1 % after 4 weeks, respectively. The maximum dough fermentation height (Hm) and final dough fermentation height (h) values of the frozen dough also exhibited notable increases of 20.2 % and 15.0 % after 2 weeks and 20.8 % and 16.6 % after 4 weeks, respectively, compared to the control. SEM was used to visualize the changes of dough microstructure during frozen storage. As shown in Fig. S4, after 2 and 4 weeks of frozen storage, the voids of frozen dough containing γ-PGA were significantly smaller than those of control samples. The frozen dough with γ-PGA also exhibited fewer exposed starch granules binding to the gluten structure than that of control.

Freezable water content, an important index affecting frozen dough quality, is closely related to the quantity of ice crystals formed during freezing (Lu et al., 2021). This study found that γ-PGA from *B.velezensis* CAU263 greatly decreased the amount of freezable water in the frozen dough. This phenomenon may occur due to the binding of γ-PGA to the surface of ice crystals, thereby inhibiting their growth. Additionally, interactions among γ-PGA, water, and gluten via hydrophobic or hydrogen bonds can convert frozen water into non-frozen water (Liu et al., 2018). These findings align with the effects of adding CMCh and WBAP to the frozen dough (Zhu et al., 2022). In this study, the

Table 3
Effects of γ-PGA on the specific volume and textural properties of frozen dough bread.

Frozen Storage Time (week)	γ-PGA (g/kg)	Special volume (mL/g)	Hardness (g)	Cohesiveness	Springiness	Resilience	Gumminess	Chewiness
2	0	3.82 ± 0.06^{e}	468.14 ± 11.26^{a}	0.77 ± 0.02^{a}	97.94 ± 3.74^{b}	36.09 ± 2.36^{b}	356.19 ± 15.38^{a}	348.87 ± 14.57^{a}
	0.1	4.02 ± 0.11^{d}	374.81 ± 22.57^{b}	0.79 ± 0.02^{a}	100.89 ± 4.65^{ab}	38.71 ± 2.87^{ab}	296.84 ± 21.12^{b}	314.41 ± 26.17^{b}
	0.2	4.15 ± 0.03^{cd}	364.73 ± 30.67^{b}	0.79 ± 0.01^{a}	101.70 ± 1.20^{ab}	39.51 ± 1.05^{a}	288.32 ± 22.87^{b}	303.40 ± 28.20^{b}
	0.3	4.18 ± 0.03^{bc}	358.37 ± 15.30^{b}	0.80 ± 0.01^{a}	103.35 ± 2.56^{ab}	40.19 ± 1.03^{a}	271.66 ± 11.00^{bc}	281.18 ± 15.85^{bc}
	0.4	4.43 ± 0.09^{a}	297.89 ± 10.35^{c}	0.80 ± 0.03^{a}	104.98 ± 1.79^{a}	40.83 ± 2.12^{a}	239.01 ± 17.26^{d}	237.64 ± 16.72^{d}
	0.5	4.32 ± 0.11^{ab}	311.15 ± 9.75^{c}	0.79 ± 0.01^{a}	98.26 ± 2.12^{b}	39.23 ± 0.94^{ab}	245.83 ± 6.33^{cd}	241.64 ± 11.21^{d}
	0.6	4.07 ± 0.11^{cd}	351.62 ± 21.19^{b}	0.77 ± 0.04^{a}	98.25 ± 2.02^{b}	37.78 ± 0.05^{ab}	271.94 ± 16.15^{bc}	267.03 ± 10.21^{cd}
4	0	3.60 ± 0.12^{c}	487.43 ± 12.56^{a}	0.76 ± 0.01^{a}	97.06 ± 1.46^{d}	35.62 ± 0.08^{c}	373.75 ± 11.99^{a}	362.76 ± 25.39^{a}
	0.1	3.88 ± 0.02^{c}	383.64 ± 3.15^{b}	0.77 ± 0.04^{a}	100.00 ± 0.82^{bcd}	38.56 ± 1.10^{abc}	302.91 ± 21.56^{b}	324.25 ± 30.44^{b}
	0.2	4.12 ± 0.03^{b}	366.78 ± 20.38^{bc}	0.77 ± 0.02^{a}	101.12 ± 1.97^{abc}	38.67 ± 1.35^{abc}	287.79 ± 18.13^{b}	291.03 ± 20.87^{bc}
	0.3	4.15 ± 0.16^{b}	360.88 ± 13.89^{bc}	0.78 ± 0.08^{a}	102.95 ± 2.58^{ab}	39.20 ± 2.16^{ab}	278.28 ± 26.79^{bc}	288.40 ± 15.44^{bc}
	0.4	4.37 ± 0.01^{a}	300.84 ± 12.18^{d}	0.79 ± 0.01^{a}	104.12 ± 2.43^{a}	40.85 ± 2.02^{a}	236.60 ± 23.88^{d}	237.34 ± 12.13^{d}
	0.5	4.30 ± 0.03^{a}	320.61 ± 10.91^{d}	0.78 ± 0.05^{a}	99.71 ± 0.25^{bcd}	37.99 ± 1.98^{abc}	248.97 ± 15.15^{cd}	241.65 ± 16.58^{d}
	0.6	4.05 ± 0.02^{b}	355.62 ± 15.24^{c}	0.77 ± 0.02^{a}	99.05 ± 1.90^{cd}	37.46 ± 1.55^{bc}	277.83 ± 17.91^{bc}	269.58 ± 19.32^{cd}

Data are expressed as mean ± standard deviation (n = 3). Values with different superscript lowercase letters in the same column of the same frozen storage time indicate significant differences ($p < 0.05$).

viscoelasticity (G' and G") decreased with increasing storage time, likely because of the recrystallization of water molecules, which mechanically damaged the gluten network (Zhu et al., 2022). However, the addition of γ-PGA significantly improved the rheological properties of frozen dough, suggesting that γ-PGA strengthens the gluten network and contributes to the formation of a sponge-like bread structure (Shu et al., 2022). The viability of yeast in frozen dough during breadmaking is of paramount importance because of the potential detrimental effects of ice crystals on yeast cell membranes, which can ultimately result in cell death (Lin et al., 2021). γ-PGA has been demonstrated to effectively protects baker's yeast from freezing induced damage during storage (Jia et al., 2016; Yokoigawa et al., 2006). In this study, γ-PGA from *B.velezensis* CAU263 significantly improved the viability of yeast in frozen dough, suggesting a cryoprotective role potentially linked to its ability to inhibit ice crystals formation (Lin et al., 2021). This study also revealed significant increases in A_T and Hm due to the presence of γ-PGA from *B. velezensis* CAU263. The quantity and activity of yeast cells are critical factors that influence the gas-producing capacity of yeast (Liu et al., 2018). γ-PGA effectively enhanced the gas production capacity of frozen dough, possibly by acting as a protective agent that preserves yeast cell membrane integrity and prevents damage to the internal structure under various freezing conditions (Jia et al., 2016; Luo et al., 2018). Furthermore, the addition of γ-PGA from *B.velezensis* CAU263 led to significant increases in the A_1, R, and h values. This can be primarily attributed to the γ-PGA strengthening of the gluten network and extensibility of frozen dough by inhibiting ice recrystallization (Jia et al., 2016). However, an excessive amount of γ-PGA disrupts the extensibility of frozen dough, resulting in the formation of a gluten network with reduced gas capturing and retention capacity (Lin et al., 2021). Therefore, γ-PGA from *B.velezensis* CAU263 showed a superior cryoprotective effect and has the potential to enhance the properties of frozen dough for bread making.

3.5. Effects of γ-PGA on frozen dough bread quality

The specific volume and textural properties of the frozen dough bread are depicted in Table 3. After 2 weeks of frozen storage, the addition of 0.4 g/kg of γ-PGA resulted in a 16.0 % increase in the specific volume of bread, along with a 36.4 % reduction in bread hardness, compared to the control. Additionally, the gumminess and chewiness decreased by 32.9 % and 31.9 %, respectively. After 4 weeks of freezing, compared to the control, the specific volume of bread increased by 21.3 %, and the hardness of bread decreased by 38.3 %. Moreover, the gumminess and chewiness reduced by 36.7 % and 34.6 %, respectively. These findings underscore the significant enhancement in textural properties of frozen dough bread attributed to γ-PGA. The quantitative visualization of water status and water distribution in frozen dough bread is shown in Table S5. After 2 and 4 weeks of frozen storage, the A_{21} value was increased by 9.7 % and 10.0 %, respectively, and the A_{23} value was decreased by 34.4 % and 36.0 %, respectively, when γ-PGA was added at 0.4 g/kg. A_{22} value was not significantly changed. The addition of γ-PGA in frozen dough bread resulted in higher A_{21} values and lower A_{23} values than those of the control, suggesting that γ-PGA could efficiently restrict water migration.

The γ-PGA sourced from *B.velezensis* CAU263 demonstrated a significant enhancement in the specific volume of frozen dough bread. γ-PGA has been recognized for its cryoprotective attributes, which effectively impedes the formation and growth of ice crystals, potentially aiding yeast survival during frozen storage (Jeong et al., 2021; Luo et al., 2018). Moreover, the water absorbing capability of γ-PGA likely contributed to the stabilization of the gluten network structure and improvement of the gas retention capacity (Liu et al., 2022). The addition of γ-PGA from *B.velezensis* CAU263 notably reduced the bread hardness. It is plausible that the presence of γ-PGA within frozen dough limits the mobility of freezable water molecules, resulting in reduced freezable water content, thereby leading to a decrease in both the number and size of ice crystals (He et al., 2020). Additionally, the addition of γ-PGA resulted in a reduction in water migration and hindered amylose aggregation (Lin et al., 2021). The γ-PGA from *B.velezensis* CAU263 had a decreased effect on bread gumminess and chewiness. Given that bread is not a very springy food, changes in gumminess and chewiness appear to be positively correlated with alterations in bread hardness (Jeong et al., 2021). Therefore, γ-PGA from *B.velezensis* CAU263 significantly improved the textural properties of the frozen dough bread. To date, there has been limited research on the application of γ-PGA in frozen dough bread. Jia et al. (2016) reported a

8.9 % increase in the specific volume of frozen dough bread after the addition of 1 % γ-PGA after 8 weeks of freezing. No other study has investigated the use of γ-PGA in frozen dough bread. These compounds such as carrot antifreeze protein (Liu et al., 2018), sweet potato protein hydrolysates (Chen, Xiao, et al., 2023), and trehalose (Gerardo-Rodriguez et al., 2017) have been reported as antifreeze in frozen dough bread. Specifically, the specific volume of bread incorporated with 0.5 % carrot antifreeze protein was increased by 19.4 %, while the hardness was decreased by 37.9 % as compared with the control group after eight freeze-thawed cycles (Liu et al., 2018). Sweet potato protein hydrolysates of 3 % have also been reported to significantly increase the specific volume of bread by 26.0 % after frozen storage for 56 d while the hardness was significantly decreased by 31.4 % (Chen, Xiao, et al., 2023). Similarly, Gerardo-Rodriguez et al. (2017) reported that the specific volume of frozen dough bread with 800 ppm trehalose was increased by 14.7 % with 37.4 % reduction in hardness. In this study, γ-PGA with addition of 0.04 % exhibited advantages in improving the quality of frozen dough bread with larger specific volume, but lower harness than those reported antifreeze additives. The findings of this study established the potential application of γ-PGA in frozen dough owing to its cryoprotective effects on bread quality. Additionally, this study serves as a foundational platform for future investigations of the cryoprotective properties of γ-PGA in various foods.

4. Conclusion

An efficient strategy for γ-PGA production through fed-batch fermentation by *B. velezensis* CAU263 was provided and its potential for frozen dough bread was evaluated. High γ-PGA yield and productivity were achieved by using a combination of six-semicircular blade Rushton turbine impeller and four-skewed wide blade impeller. The purified γ-PGA exhibited a Mw of 3.3×10^6 Da and an L-glutamic acid content of 42.5 %. When incorporated into frozen dough, γ-PGA effectively reduced the content of freezable water and improved the rheological properties of frozen dough. Besides, the survival rate of yeast was increased as well as the fermentation height of frozen dough. As a result, the γ-PGA-added bread exhibited larger specific volume, lower hardness, and better texture. Hence, γ-PGA that produced by *B. velezensis* CAU263 has promising potential of applications in baking industry.

CRediT authorship contribution statement

Hong Liu: Writing – review & editing, Methodology, Conceptualization. **Qiaojuan Yan:** Writing – original draft, Investigation, Funding acquisition. **Yuchuan Wang:** Software, Data curation. **Yanxiao Li:** Visualization, Project administration. **Zhengqiang Jiang:** Writing – review & editing, Supervision.

Declaration of competing interest

The authors declare that they have no known competing financial interests or personal relationships that could have appeared to influence the work reported in this paper.

Acknowledgement

This work was supported by the National Key Research and Development Program of China (No. 2022YFD2101400).

Appendix A. Supplementary data

Supplementary data to this article can be found online at https://doi.org/10.1016/j.fochx.2025.102247.

Data availability

Data will be made available on request.

References

Abdelnaby, T., Li, Z. J., & Xue, C. H. (2024). The influence of γ-PGA on the quality of cooked frozen crayfish during temperature fluctuations. *Food Chemistry, 441, Article 138258*.

Ali, A. A. M., Momin, B., & Ghogare, P. (2020). Isolation of a novel poly-γ-glutamic acid-producing *Bacillus licheniformis* A14 strain and optimization of fermentation conditions for high-level production. *Preparative Biochemistry & Biotechnology, 50*(5), 445–452.

Bernauer, S., Eibl, P., Witz, C., Khinast, J., & Hardiman, T. (2022). Analyzing the effect of using axial impellers in large-scale bioreactors. *Biotechnology and Bioengineering, 119*(9), 2494–2504.

Chen, H., Yi, X. G., Zhang, X. B., & Luo, Z. H. (2023). CFD-PBM simulation and scale-up of the pilot-scale bioreactor. *Industrial & Engineering Chemistry Research, 62*(1), 741–752.

Chen, J. R., Xiao, J. H., Tu, J., Yu, L. L., & Niu, L. Y. (2023). The alleviative effect of sweet potato protein hydrolysates on the quality deterioration of frozen dough bread in comparison to trehalose. *LWT - Food Science and Technology, 175, Article 114505*.

Elbanna, K., Alsulami, F. S., Neyaz, L. A., & Abulreesh, H. H. (2024). Poly (γ) glutamic acid: A unique microbial biopolymer with diverse commercial applicability. *Frontiers in Microbiology, 15, Article 1348411*.

Fukushima, T., Uchida, N., Ide, M., Kodama, T., & Sekiguchi, J. (2018). DL-endopeptidases function as both cell wall hydrolases and poly-γ-glutamic acid hydrolases. *Microbiology-SGM, 164*(3), 277–286.

Gerardo-Rodriguez, J. E., Ramirez-Wong, B., Ledesma-Osuna, A. I., Medina-Rodriguez, C. L., Ortega-Ramirez, R., & Silvas-Garcia, M. I. (2017). Management of freezing rate and trehalose concentration to improve frozen dough properties and bread quality. *Food Science and Technology, 37*(1), 59–64.

Guo, Y., Liu, Y. Y., Yang, Z. J., Chen, G. G., Liang, Z. Q., & Zeng, W. (2024). Enhanced production of poly-γ-glutamic acid by *Bacillus subtilis* using stage-controlled fermentation and viscosity reduction strategy. *Applied Biochemistry and Biotechnology, 196*(3), 1527–1543.

Halmschlag, B., Steurer, X., Putri, S. P., Fukusaki, E., & Blank, L. M. (2019). Tailor-made poly-γ-glutamic acid production. *Metabolic Engineering, 55*, 239–248.

He, Y. J., Guo, J. Y., Ren, G. Y., Cui, G. T., Han, S. H., & Liu, J. X. (2020). Effects of konjac glucomannan on the water distribution of frozen dough and corresponding steamed bread quality. *Food Chemistry, 330, Article 127243*.

Huang, J., Du, Y. M., Xu, G. H., Zhang, H. L., Zhu, F., Huang, L., & Xu, Z. N. (2011). High yield and cost-effective production of poly (γ-glutamic acid) with *Bacillus subtilis*. *Engineering in Life Sciences, 11*(3), 291–297.

Jeong, S. M., Park, Y. J., & Lee, S. Y. (2021). Assessment of turanose as a sugar alternative in a frozen dough system: Rheology, tomography, and baking performance. *LWT - Food Science and Technology, 141, Article 110869*.

Jia, C. L., Huang, W. N., Tang, X. J., Ding, S. S., Yang, W. D., Li, Z. B., … Rayas-Duarte, P. (2016). Antifreeze activity of γ-poly glutamic acid and its impact on freezing resistance of yeast and frozen sweet dough. *Cereal Chemistry, 93*(3), 306–313.

Jiang, Y. X., Tang, B., Xu, Z. Q., Liu, K., Xu, Z., Feng, X. H., & Xu, H. (2016). Improvement of poly-γ-glutamic acid biosynthesis in a moving bed biofilm reactor by *Bacillus subtilis* NX-2. *Bioresource Technology, 218*, 360–366.

Kongklom, N., Shi, Z. P., Chisti, Y., & Sirisansaneeyakul, S. (2017). Enhanced production of poly-γ-glutamic acid by *Bacillus licheniformis* TISTR 1010 with environmental controls. *Applied Biochemistry and Biotechnology, 182*, 990–999.

Li, D. F., Hou, L. Z., Gao, Y. X., Tian, Z. L., Fan, B., Wang, F. Z., & Li, S. Y. (2022). Recent advances in microbial synthesis of poly-γ-glutamic acid: A review. *Foods, 11*(5), 739.

Li, J., Chen, S. B., Fu, J. M., Xie, J. C., Ju, J. S., Yu, B., & Wang, L. M. (2022). Efficient molasses utilization for low-molecular-weight poly-γ-glutamic acid production using a novel *Bacillus subtilis* strain. *Microbial Cell Factories, 21, Article 140*.

Lin, J. J., Sun-Waterhouse, D. X., Tang, R. M., Cui, C., Wang, W., & Xiong, J. (2021). The effect of γ-$[Glu]_{(1\leq n\leq 5)}$-Gln on the physicochemical characteristics of frozen dough and the quality of baked bread. *Food Chemistry, 343, Article 128406*.

Liu, H., Yan, Q. J., Wang, Y. C., Li, Y. X., & Jiang, Z. Q. (2022). Efficient production of poly-γ-glutamic acid by *Bacillus velezensis* via solid-state fermentation and its application. *Food. Bioscience, 46, Article 101575*.

Liu, M., Liang, Y., Zhang, H., Wu, G. C., Wang, L., Qian, H. F., & Qi, X. G. (2018). Production of a recombinant carrot antifreeze protein by *Pichia pastoris* GS115 and its cryoprotective effects on frozen dough properties and bread quality. *LWT - Food Science and Technology, 96*, 543–550.

Lu, L., Yang, Z., Guo, X. N., Xing, J. J., & Zhu, K. X. (2021). Effect of $NaHCO_3$ and freeze-thaw cycles on frozen dough: From water state, gluten polymerization and microstructure. *Food Chemistry, 358, Article 129869*.

Luo, W. H., Sun, D. W., Zhu, Z. W., & Wang, Q. J. (2018). Improving freeze tolerance of yeast and dough properties for enhancing frozen dough quality-a review of effective methods. *Trends in Food Science & Technology, 72*, 25–33.

Min, J. H., Reddy, L. V., Charalampopoulos, D., Kim, Y. M., & Wee, Y. J. (2019). Optimized production of poly (γ-glutamic acid) by *Bacillus* sp. FBL-2 through response surface methodology using central composite design. *Journal of Microbiology and Biotechnology, 29*(7), 1061–1070.

Nadal-Rey, G., McClure, D. D., Kavanagh, J. M., Cassells, B., Cornelissen, S., Fletcher, D. F., & Gernaey, K. V. (2022). Computational fluid dynamics modelling of

hydrodynamics, mixing and oxygen transfer in industrial bioreactors with Newtonian broths. *Biochemical Engineering Journal, 177, Article 108265*.
Nair, P., Navale, G. R., & Dharne, M. S. (2023). Poly-gamma-glutamic acid biopolymer: A sleeping giant with diverse applications and unique opportunities for commercialization. *Biomass Conversion and Biorefinery, 13*(6), 4555–4573.
Parati, M., Khalil, I., Magaia, F. T., Adamus, G., Mendrek, B., Hill, R., & Radecka, I. (2022). Building a circular economy around poly (D/L-γ-glutamic acid)- a smart microbial biopolymer. *Biotechnology Advances, 61, Article 108049*.
Peng, Y. Y., Jiang, B., Zhang, T., Mu, W. M., Miao, M., & Hua, Y. F. (2015). High-level production of poly (γ-glutamic acid) by a newly isolated glutamate-independent strain. *Bacillus methylotrophicus. Process Biochemistry, 50*(3), 329–335.
Qiu, Y. B., Sha, Y. Y., Zhang, Y. T., Xu, Z. Q., Li, S., Lei, P., … Xu, H. (2017). Development of Jerusalem artichoke resource for efficient one-step fermentation of poly-(γ-glutamic acid) using a novel strain *Bacillus amyloliquefaciens* NX-2S. *Bioresource Technology, 239*, 197–203.
Ratha, P., & Jhon, D. Y. (2019). Factors increasing poly-γ-glutamic acid content of cheongguk-jang fermented by *Bacillus subtilis* 168. *Food Science and Biotechnology, 28*(1), 103–110.
Sha, Y. Y., Zhang, Y. T., Qiu, Y. B., Xu, Z. Q., Li, S., Feng, X. H., … Xu, H. (2019). Efficient biosynthesis of low-molecular-weight poly-γ-glutamic acid by stable overexpression of PgdS hydrolase in *Bacillus amyloliquefaciens* NB. *Journal of Agricultural and Food Chemistry, 67*(1), 282–290.
Shu, Q., Wei, T. Y., Liu, X. Y., Liu, S. Y., & Chen, Q. H. (2022). The dough-strengthening and spore-sterilizing effects of mannosylerythritol lipid-a in frozen dough and its application in bread making. *Food Chemistry, 369, Article 131011*.
Sirisansaneeyakul, S., Cao, M. F., Kongklom, N., Chuensangjun, C., Shi, Z. P., & Chisti, Y. (2017). Microbial production of poly-γ-glutamic acid. *World Journal of Microbiology & Biotechnology, 33*(9), 173.
Song, D. Y., Reddy, L. V., Charalampopoulos, D., & Wee, Y. J. (2019). Poly-(γ-glutamic acid) production and optimization from agro-industrial bioresources as renewable substrates by *Bacillus* sp. FBL-2 through response surface methodology. *Biomolecules, 9*(12), 754.
Tian, G. M., Fu, J. T., Wei, X. T., Ji, Z. X., Ma, X., Qi, G. F., & Chen, S. W. (2014). Enhanced expression of *pgdS* gene for high production of poly-γ-glutamic acid with lower molecular weight in *Bacillus licheniformis* WX-02. *Journal of Chemical Technology and Biotechnology, 89*(12), 1825–1832.
Verma, R., Mehan, L., Kumar, R., Kumar, A., & Srivastava, A. (2019). Computational fluid dynamic analysis of hydrodynamic shear stress generated by different impeller combinations in stirred bioreactor. *Biochemical Engineering Journal, 151, Article 107312*.
Wang, D. X., Kim, H., Lee, S., Kim, D. H., & Joe, M. H. (2020). High-level production of poly-γ-glutamic acid from untreated molasses by *Bacillus siamensis* IR10. *Microbial Cell Factories, 19(1), Article 101*.
Wang, L. M., Chen, S. B., & Yu, B. (2022). Poly-γ-glutamic acid: Recent achievements, diverse applications and future perspectives. *Trends in Food Science & Technology, 119*, 1–12.
Yang, Z. X., Xu, D., Zhou, H. L., Wu, F. F., & Xu, X. M. (2022). New insight into the contribution of wheat starch and gluten to frozen dough bread quality. *Food. Bioscience, 48, Article 101777*.
Yokoigawa, K., Sato, M., & Soda, K. (2006). Simple improvement in freeze-tolerance of bakers' yeast with poly-γ-glutamate. *Journal of Bioscience and Bioengineering, 102*(3), 215–219.
Zeng, W., Liang, Z. Q., Li, Z., Bian, Y. X., Li, Z. H., Tang, Z., & Chen, G. G. (2016). Regulation of poly-γ-glutamic acid production in *Bacillus subtilis* GXA-28 by potassium. *Journal of the Taiwan Institute of Chemical Engineers, 61*, 83–89.
Zeng, W., Liu, Y. Y., Shu, L., Guo, Y., Wang, L. Y., & Liang, Z. Q. (2024). Production of ultra-high-molecular-weight poly-γ-glutamic acid by a newly isolated *Bacillus subtilis* strain and genomic and transcriptomic analyses. *Biotechnology Journal, 19*(4), Article e202300614.
Zhu, X. W., Yuan, P. P., Zhang, T., Wang, Z. K., Cai, D. N., Chen, X., … Goff, D. (2022). Effect of carboxymethyl chitosan on the storage stability of frozen dough: State of water, protein structures and quality attributes. *Food Research International, 151, Article 110863*.